J. Phys. B: At. Mol. Opt. Phys. 24 (1991) 473-487. Printed in the UK

Absolute elastic differential cross sections for electron scattering from SF_6

W M Johnstone and W R Newell

Department of Physics and Astronomy, University College London, Gower Street, London WC1E 6BT, UK

Received 31 May 1990, in final form 1 November 1990

Abstract. A conventional hemispherical electron spectrometer has been used to measure absolute cross sections for elastic scattering of electrons from SF_6 for incident electron energies between 5 and 75 eV and for scattering angles 10° to 120°. Absolute integral and momentum transfer cross sections have also been determined from an extrapolation of the differential cross section data. The reported cross sections are in good agreement with the other relevant data, both experimental and theoretical. Evidence is also seen for resonance enhancement of the cross section at 7.2 and 12 eV.

1. Introduction

There are several applications where the cross sections for electron scattering from sulphur hexafluoride (SF_6) are of considerable interest. In particular, as the feature sizes of very large scale integrated circuits are reduced to the sub-micron level, dry plasma etching techniques are gradually replacing wet chemical etching methods (Endo and Kurogi 1980, Pinto *et al* 1987). This is due to the ability of the dry etching process to give anisotropic and highly directional vertical etch profiles with good selectivity. SF_6 is also widely used as a gaseous dielectric where high-voltage breakdown is a problem (Christophorou *et al* 1982). Since SF_6 has a very large cross section (5.2×10^{-14} cm^2, Chutjian 1981) for the formation of SF_6^- at near-zero electron energies, any low-energy electrons are 'mopped up' before they have a chance to create an avalanche breakdown. To obtain better control in both these situations, plasma models and electron-transport equations require a comprehensive set of electron-impact cross section data. Elastic cross sections are also necessary for normalizing the corresponding inelastic processes.

The number of differential cross section (DCS) measurements reported for electron scattering from SF_6 are limited and the data are by no means conclusive. Absolute elastic measurements have been made by Rohr (1979) for incident electron energies from 0.05 to 10 eV and for scattering angles between $\theta = 20°$ and 120°, Srivastava *et al* (1976) for incident energies between 5 and 75 eV and scattering angles from $\theta = 20°$ to 135° and Sakae *et al* (1989) for energies between 75 and 700 eV and $\theta = 5°$ to 135°. Trajmar and Chutjian (1977) have made relative measurements for incident energies between 9 and 17 eV for 20°, 60°, 90° and 135° scattering angles. The present work is an independent study of e–SF_6 scattering which spans the previous studies to ensure good validation. A preliminary account of this work has already been reported by Johnstone and Newell (1989).

0953-4075/91/020473+15$03.50

2. Experimental details

2.1. The spectrometer

A schematic diagram of the spectrometer is shown in figure 1. The monochromator produces a collimated monoenergetic electron beam which is crossed at 90° with a gas beam directed perpendicularly into the plane of figure 1. Electrons scattered in the plane perpendicular to the gas beam are detected by an analyser and a reference detector. The analyser can detect electrons scattered at angles between $\theta = -10°$ and 120° while the reference detector measures the scattered electron flux at a fixed angle of $\theta = -90°$. The electron spectrometer used in this work has not been previously discussed in the literature, so a brief description of its various components is given below.

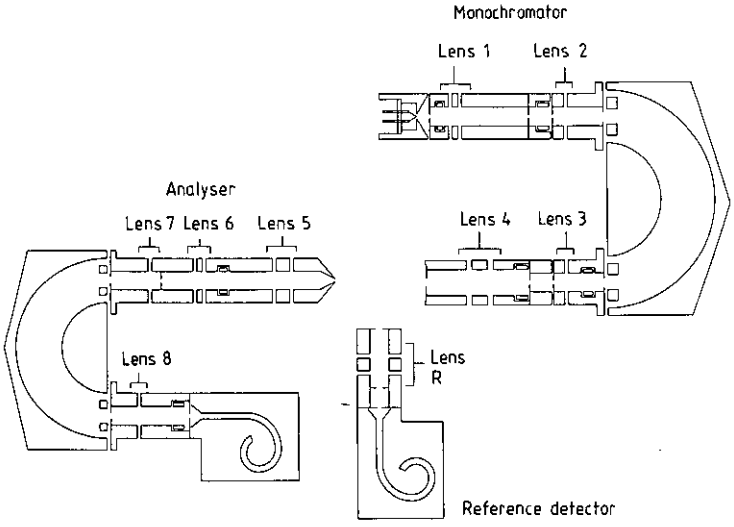

Figure 1. A schematic diagram of the spectrometer. The analyser is positioned at the scattering angle $\theta = 0°$, while the reference detector is fixed at $\theta = -90°$. See text for a full discussion.

Electrons emitted from a thoriated tungsten hairpin filament in a Pierce configuration, are focused by lenses 1 and 2 to the entrance of a hemispherical monochromator. Proper attention has been paid to the positioning of windows and pupils in the electron gun such that the divergence of the electron beam at the entrance of the monochromator is reduced to a minimum. Only those electrons whose energy falls in a narrow energy band are transmitted by the monochromator and the emergent electron beam is focused by lenses 3 and 4 to the centre of an interaction region where it intersects the gas beam. Typical currents and energy spreads obtainable range between 2 nA for a full width half maximum (FWHM) of 20 meV to 50 nA for 80 meV FWHM. The angular divergence of the beam is 2° and the beam diameter is 1 mm in the interaction region.

The analyser is of a similar design to the monochromator. Electrons scattered through an angle θ are focused by lenses 5, 6 and 7 into a hemispherical analyser. Again, only those electrons in a certain energy range are transmitted through the hemispheres where they are subsequently detected by a channel electron multiplier (CEM). Both the monochromator and the analyser employ concentric hoops to correct

for fringing fields at their entrance and exit. The best resolution obtained from the spectrometer was 28 meV, although it usually operated with a resolution between 50–60 meV with larger beam currents to reduce the data collection time. The contact potential is determined by observing the position of the 19.36 eV helium resonance and comparing it to the value quoted by Brunt *et al* (1977).

The reference detector is a three-element filter lens (lens R) followed by a CEM. Its purpose is to measure the scattered electron flux at a fixed angle of $\theta = -90°$. By applying a sufficiently negative voltage to the centre element of the lens, it is possible to select only those electrons that have been elastically scattered from the gas beam. To ensure that the reference detector maintains a constant scattering angle it is attached to the monochromator section.

The gas beam is formed by flowing gas through a capillary tube 25 mm long with an internal diameter of 0.6 mm. It is held at the centre of an interaction-region cylinder which provides an electrostatic-field-free region in which the electrons can scatter from the gas beam. Slots and apertures cut into the cylinder allow the incident beam to enter and scattered electrons to leave. The interaction-region assembly is mounted on the monochromator section which ensures that the position of the gas beam remains constant with respect to the incident electron beam.

The monochromator assembly (including the reference detector and interaction region) is attached to a rotating arm mechanism allowing it to be rotated about the gas beam axis while the analyser remains stationary. Great care is taken in aligning the monochromator and the analyser with respect to the interaction region, as any error could introduce a false angular dependence in the measured cross section.

The spectrometer is housed in a vacuum chamber pumped by a liquid nitrogen trapped-oil diffusion pump and it is periodically heated using an internally fitted projector lamp bulb. The base pressure in the vacuum chamber is better than 1×10^{-7} Torr. Non-magnetic materials are used in the construction of the spectrometer which is enclosed in a mu-metal container. This reduces the residual field in the chamber to less than 10 mG.

2.2. Experimental method

In this work the absolute DCS are measured in two stages. First, the relative differential cross sections are determined at the desired impact energy and for scattering angles between $\theta = 10°$ and 120° using the subtraction technique (described in section 2.2.1). The absolute value of the cross section is then measured at $\theta = 90°$ using the relative flow technique (described in section 2.2.2) and this value is then used to normalize the corresponding relative DCS. This approach was employed because a prerequisite of the relative flow technique is being able to measure the incident electron beam flux. Due to severe mechanical problems a Faraday cup could not be fitted to the spectrometer and the only angle at which the electron beam could be measured was $\theta = 90°$.

2.2.1. Determination of the relative cross section. A major problem associated with electron scattering experiments is ensuring the long term stability of both the electron and gas beams. This is particularly important when making comparisons between measurements made at different scattering angles, as one needs to ensure that any changes observed are a result of a change in the cross section and not a change in intensity of either the gas or electron beam. The scattered electron count rate is proportional to I_0 (the incident electron beam current) and ρ (the gas beam density).

If it were possible to measure the product $I_o\rho$ while simultaneously measuring the scattered electron count rate then any variations in the count rate due to fluctuations in the gas or electron beam could be accounted for.

In the present work this is achieved by using a reference detector placed at a fixed scattering angle of $\theta = -90°$ (see figure 1). The scattered electron flux monitored by this detector is proportional to $I_o\rho$. Hence each time a count rate is recorded by the analyser at any angle θ it is normalized to the simultaneously measured count rate obtained from the reference detector. Thus if $D(\theta)$ is the count rate recorded by the analyser and $R(\theta)$ is the count rate simultaneously recorded by the reference detector then the ratio of the cross sections $\sigma(\theta)/\sigma(-90°)$ is given by

$$\sigma(\theta)/\sigma(90°) = \frac{D(\theta)R(90°)V_{\text{eff}}(90°)}{D(90°)R(\theta)V_{\text{eff}}(\theta)} \tag{1}$$

where σ is the differential cross section and $(V_{\text{eff}}(90°)/V_{\text{eff}}(\theta))$ is the effective path length or volume correction associated with the overlapping beam geometry. Any change in $D(\theta)$ due to a variation in gas pressure or electron beam current is corrected for in the ratio $R(90°)/R(\theta)$. In using equation (1) it is assumed that the only source of electrons were those scattered from the gas beam. In reality there are significant contributions to the analyser and reference detector count rates from other sources. When the gas is beamed into the system through the capillary tube the background pressure in the tank rises and electrons scattered from this background gas (or gas cell) will contribute to the observed count rates in both the analyser and the reference detector. This contribution must be removed as the scattering volume of the electron beam and the gas cell is different to that between the electron beam and the gas beam. The other major contribution to the measured count rates comes from electrons scattered from the surfaces in and around the interaction region.

Hence the count rate measured by the analyser (D_{bc}) and the reference detector (R_{bc}) in the 'beam plus cell' configuration contains three separate contributions and is given by

$$D_{\text{bc}}(\theta) \propto I_o[(V_{\text{beff}}(\theta)\rho_b + V_{\text{ceff}}(\theta)P_c)\sigma(\theta) + S_D(\theta)] \tag{2}$$

$$R_{\text{bc}}(\theta) \propto I_o[(\rho_b + P_c)\sigma(90°) + S_R(\theta)] \tag{3}$$

where ρ_b represents the gas beam density, P_c the cell density and $S_D(\theta)$ and $S_R(\theta)$ are contributions from electrons scattered from surfaces into the analyser and the reference detector respectively. In the case of a 'cell only' configuration the measured count rates are given by

$$D_c(\theta) \propto I'_o[V_{\text{ceff}}(\theta)P_c\sigma(\theta) + S_D(\theta)] \tag{4}$$

and

$$R_c(\theta) \propto I'_o[P_c\sigma(\theta) + S_R(\theta)] \tag{5}$$

where allowance has been made for the possible change in the electron beam current. Combining equations (2) and (3) with (4) and (5) yields the following expressions for D and R

$$D(\theta) = D_{\text{bc}}(\theta) - (I_o/I'_o)D_c(\theta) \propto I_o[V_{\text{beff}}(\theta)\rho_b\sigma(\theta)] \tag{6}$$

$$R(\theta) = R_{\text{bc}}(\theta) - (I_o/I'_o)R_c(\theta) \propto I_o[\rho_b\sigma(\theta)]. \tag{7}$$

Using equations (6) and (7), equation (1) can be rewritten as

$$\frac{\sigma(\theta)}{\sigma(90)} = \frac{D_{\text{bc}}(\theta) - (I_o/I'_o)D_c(\theta)R_{\text{bc}}(90°) - (I_o/I'_o)R_c(90°)F_{\text{eff}}(\theta)}{D_{\text{bc}}(90°) - (I_o/I'_o)D_c(90°)R_{\text{bc}}(\theta) - (I_o/I'_o)R_c(\theta)} \tag{8}$$

where $F_{eff}(\theta) = V_{eff}(\theta)/V_{eff}(90°)$. In obtaining equation (8) two assumptions have been made. The first is that P_c is the same when making beam plus cell and cell measurements. This is easily achieved by adjusting the flow rate of gas into the chamber. The second is that the electron beam profile is independent of small changes in current. The most likely cause of any change in the current is a variation in the emission from the filament or a change in the transmission of the monochromator. Neither of these effects is likely to alter the focusing of the beam at the interaction region by lens 4. Also, as the magnitude of the incident beam current is of the order of 10 s of nA, the profile is unlikely to be altered by space charge effects.

The experimental process implied in the derivation of equation (8) is that two experiments are performed. Firstly, a measurement of the DCS is made for a beam plus cell configuration with an incident electron beam current I_o. A second DCS is then measured for a cell only configuration with an incident electron beam current I'_o and where the cell pressure P_c has been adjusted to be the same as in the beam plus cell measurement. If the results of the second experiment are normalized to the first by taking account of any difference between I_o and I'_o, then the results of the second experiment can be subtracted from the first and the effect of the background gas and surface scattering will be removed. This technique was first used by Andrick and Bitsch (1975) and is known as the subtraction technique. The derivation of equations (2) to (8) are based on a refinement of this technique by Newell *et al* (1981).

$F_{eff}(\theta)$ is determined by measuring the relative DCS for a gas where the value of the DCS is already well documented. The gas chosen for this task is helium as there exists a large amount of data, both theoretical and experimental, for elastic scattering of electrons from helium for a large range of energies. For incident beam energies less than 20 eV the data of Nesbet (1979) is used as a reference. This data is in the form of theoretically determined phaseshifts which allow the elastic cross section to be calculated at any angle and any energy below the first excited state. For energies of 20 eV and above the experimental data of Register *et al* (1980) is used. Having determined $F_{eff}(\theta)$, the procedure was repeated with SF_6 and the relative DCS, corrected with $F_{eff}(\theta)$, determined.

2.2.2. The determination of the absolute cross section at 90°. The relative flow technique for measuring absolute elastic differential cross sections from gaseous targets was first described by Srivastava *et al* (1975). Since then, the technique has been developed by a number of authors and has recently been reviewed by Nickel *et al* (1989). Using this technique the unknown elastic DCS for a gas 1 is determined by comparing the scattered electron flux from gas 1, $I_1^e(E_o, \theta)$, to the scattered electron flux from a second gas 2, $I_2^e(E_o, \theta)$, whose cross section for the incident energy E_o and scattering angle θ is already well known. It is assumed that the electron beam flux distribution, the angular distribution of the gas beam and the detection efficiency remain the same for both measurements.

The major difficulty in using the relative flow technique is ensuring that the angular distributions of the two gas beams are equal. When the gas beam is produced by a capillary tube Trajmar and Register (1984) have shown that the resultant angular distribution will be the same for the two gases if their Knudsen numbers (K_{nd}) are equal as the gas enters the tube. The Knudsen number K_{nd}, is given by (λ/d), where λ $(=(1/2)^{1/2}\pi n\delta^2)$ is the mean free path, n is the gas density at the entrance of the tube and δ is the molecular diameter. Equal values for K_{nd} implies equal values of λ. For a capillary of length L and diameter d where $L \gg d$, the range of validity of the

above assumption is $1 < K_{nd} < 10L/d$. Nickel *et al* (1989) have shown that provided the above criteria are satisfied then

$$\frac{I_1^e(E_o, \theta)}{I_2^e(E_o, \theta)} = \frac{\sigma_1(E_o, \theta) N_1 m_1^{1/2}}{\sigma_2(E_o, \theta) N_2 m_2^{1/2}} \tag{9}$$

where N_1 and N_2 are the flow rates of the two gases through the tube, σ_1 and σ_2 are the corresponding elastic cross sections of the two gases and m_1 and m_2 are the molecular masses of the two gases. To account for any changes in the electron beam current between the measurement of I_1^e and I_2^e, Kanik *et al* (1989) have suggested adding a current term to equation (9) giving

$$\frac{I_1^e(E_o, \theta)}{I_2^e(E_o, \theta)} = \frac{\sigma_1(E_o, \theta) N_1 I_{o1} m_1^{1/2}}{\sigma_2(E_o, \theta) N_2 I_{o2} m_2^{1/2}} \tag{10}$$

where I_{o1} and I_{o2} are the incident electron beam currents. In the spectrometer used in this work, the electrons scattered from the gas beam can be measured with two detectors; an analyser and a reference detector. By tuning the spectrometer in the zero-angle position, the primary beam can be collected and measured by the analyser. The reference detector can then be used to monitor the scattered electron flux at −90°.

The experimental procedure used is as follows. Helium (the calibration gas) is admitted to the system via the capillary tube and the pressure in the source reservoir adjusted so that the mean free path of the helium atoms in the reservoir is equal to the capillary tube diameter. The contact potential of the electron beam is determined and the incident beam energy is set to the desired value (corrected for the contact potential). The primary electron beam is collected by the analyser and measured on the outer analysing hemisphere. The reference detector is then tuned to detect electrons elastically scattered from the gas beam. The scattered electron count rate (I_{b2}^e) is then measured in addition to the pressure behind the capillary tube (P_2) and the electron beam current reaching the outer analysing hemisphere (I_{o2}). The count rate is measured for a time period that ensures that the statistical accuracy is better than 2%. The helium is then diverted from the capillary tube to a side leak in the vacuum chamber wall and the flow adjusted such that the background pressure in the chamber remains unchanged. The scattered electron count rate is again measured (I_{c2}^e). The purpose of this second measurement is to measure the number of electrons scattered from sources other than the gas beam, e.g. the background gas in the chamber. The helium gas is then pumped away and replaced by SF_6 and the procedure is repeated. The pressure behind the capillary tube, P_1, is again adjusted such that the mean free path of the molecules in the source reservoir is equal to the diameter of the capillary tube. This ensures that the Knudsen number in the source reservoir for the two gases is the same and therefore the relative density distributions of the gas beams at the exit of the capillary tube are the same. With the gas beam present the recorded count rate, reservoir pressure and electron beam current are I_{b1}^e, P_1 and I_{o1} respectively. For the background measurement the recorded count rate is I_{c1}^e. Thus from equation (10)

$$\frac{\sigma_1(E, \theta)}{\sigma_2(E, \theta)} = \frac{(I_{b1}^e - I_{c1}^e) N_2 I_{o2} m_2^{1/2}}{(I_{b2}^e - I_{c2}^e) N_1 I_{o1} m_1^{1/2}}. \tag{11}$$

To determine the *ratio* of the flow rates for the two gases used in this work a method described by Khakoo and Trajmar (1986) is used.

Having determined the absolute section at 90°, this value is used to normalize the relative differential cross sections to an absolute scale. Finally the differential cross

sections are extrapolated to 0° and 180° using a least-squares fitting function based on a Legendre polynomial expansion. This enables the integral and momentum transfer cross sections to be determined.

2.3. Error determination

The errors in the absolute cross sections arise from several sources and can be divided into two groups; those occurring in the measurement of the relative DCS and those from the determination of the absolute DCS at 90°. For the relative SF_6 DCS measurements the first source of error is from the determination of $F_{eff}(\theta)$. This involves measuring a helium DCS and then calculating the correction required to bring it into line with previously published helium DCS data. Therefore, the error in $F_{eff}(\theta)$ comes

Table 1. Absolute elastic differential cross sections for electron scattered from SF_6 ($\times 10^{-16}$ cm^2 sr^{-1}).

θ	5.0 eV	7.2 eV	10 eV	12 eV	15 eV	20 eV	30 eV	40 eV	50 eV	75 eV
0°	—	—	—	—	—	—	—	—	—	—
10°	—	—	5.00	20.05	7.75	—	12.62	16.22	15.62	16.90
15°	—	8.19	4.80	15.30	6.55	9.56	9.95	10.21	9.61	8.70
20°	2.26	7.02	4.46	12.32	5.44	5.92	7.23	6.23	4.35	2.94
25°	2.35	6.54	3.93	9.20	4.83	4.29	4.00	2.61	1.77	1.18
30°	2.44	5.64	3.56	7.17	3.86	2.85	1.94	1.18	1.12	1.26
35°	2.43	4.76	3.03	4.68	2.90	1.72	1.04	0.81	1.05	1.30
40°	2.29	3.82	2.30	3.12	1.87	1.00	0.90	0.83	1.04	1.11
45°	2.13	2.98	1.63	1.95	1.14	0.60	1.01	1.00	0.95	0.84
50°	2.00	2.20	1.20	1.36	0.77	0.60	1.20	1.03	0.88	0.56
55°	1.74	1.58	0.86	0.80	0.67	0.77	1.35	0.96	0.73	0.44
60°	1.44	1.15	0.73	0.62	0.81	1.04	1.28	0.79	0.53	0.29
65°	1.15	0.87	0.75	0.80	0.96	1.21	1.15	0.58	0.36	0.28
70°	0.95	0.78	0.88	0.96	1.09	1.28	0.96	0.41	0.24	0.23
75°	0.79	0.79	1.01	1.26	1.19	1.31	0.74	0.26	0.16	0.21
80°	0.69	0.91	1.11	1.35	1.15	1.20	0.55	0.17	0.15	0.20
85°	0.71	1.06	1.19	1.42	1.16	1.03	0.42	0.17	0.21	0.20
90°	0.74	1.32	1.17	1.44	0.99	0.81	0.35	0.20	0.23	0.17
95°	0.81	1.41	1.04	1.44	0.89	0.68	0.35	0.27	0.26	0.15
100°	0.91	1.37	0.90	1.37	0.76	0.59	0.44	0.34	0.29	0.15
105°	1.00	1.27	0.78	1.25	0.69	0.55	0.52	0.42	0.30	0.14
110°	1.04	1.14	0.64	1.28	0.65	0.55	0.59	0.46	0.34	0.16
115°	1.06	1.05	0.61	1.31	0.64	0.61	0.62	0.48	0.38	0.23
120°	1.04	0.93	0.61	1.51	0.64	0.72	0.66	0.52	0.43	0.27
error	12.0%	12.0%	12.0%	14.0%	12.0%	12.0%	13.0%	12.5%	12.5%	13.0%

Table 2. Absolute integral and momentum transfer cross sections for electrons scattered from SF_6 ($\times 10^{-16}$ cm^2).

σ_i	15.08	22.72	19.41	28.26	17.07	18.10	16.41	12.38	11.23	9.37
	17%	23%	24%	13%	17%	35%	21%	15%	16%	21%
σ_m	12.11	16.11	12.68	17.62	12.26	14.73	11.40	6.94	6.01	5.13
	33%	40%	42%	36%	42%	55%	53%	50%	51%	66%

from the counting errors in the signal from the analyser and the reference detector (4%) and the measurement of the electron beam current (2%) and gas pressure (2%). To this is added the accuracy of the published helium cross sections giving the error in $F_{\text{eff}}(\theta)$ as 7%. The measurement errors associated with the SF_6 DCS are the same as those for helium excepting those derived from the published helium data. Thus the total error in the relative SF_6 DCS is 9%.

For the absolute cross section measurements made at 90°, the sources of experimental uncertainties arise from the measurement of the flow rate (5%) and errors in the current measurement (2%). The error in the scattered electron signal contains two contributions, statistical counting errors (3%) and a contribution from inelastically scattered electrons. As a result of the low resolution of the reference detector ($\simeq$100 meV), a small proportion of the measured electron count rate may have been due to the detection of inelastically scattered electrons which had excited vibrational energy levels in the SF_6 molecule. SF_6 was found to have a vibrational excitation cross section which was at most 2% of the elastic cross section at 90° for the non-resonant energies studied in this work (Trajmar and Chutjian 1977). However, at incident electron energies of 12 eV the ratio of vibrational excitation and elastic cross sections was seen to rise to 5% (Trajmar and Chutjian 1977). Therefore, the total error in the relative intensities measured by the reference detector was found to vary between 6% and 8% depending on the incident energy and the target. The error on the absolute helium cross section at 90° used, varied between 5% and 7%. Thus, the errors in the absolute measurements were calculated to be between 8% and 11%. Therefore, the final error in any absolute differential cross section measured in this work was found to be between 12% and 14%. The errors in the integral and momentum transfer cross sections are probably higher due to errors in the extrapolation of the DCS to 0° and 180°. Because of this we ascribe an error of 17% to the integral cross section (σ_t) measurements and 20% to the momentum transfer cross section (σ_m). All the DCS values are listed in table 1 and the values for σ_t and σ_m are given in table 2. The numbers shown as percentages in table 2 represent the contribution from the extrapolated values to the final value of the cross section.

3. Results and discussion

3.1. Differential cross sections

The results of the present work have been tabulated in table 1 and the DCS are shown in figures 2 to 4. The data of Srivastava *et al* (1976), Rohr (1979), and Sakae *et al* (1989) are also shown for comparison. The data of Srivastava *et al* (1976) have been recalculated using the improved helium cross sections of Register (1980) and the data shown are those given by Trajmar *et al* (1983).

Figure 2(*a*) shows the data taken at 5 eV and the trend of the present data is in qualitative agreement with the data of Rohr (1979) and Srivastava *et al* (1976) for scattering angles $\theta \geqslant 50°$. For $\theta < 50°$ the data of Srivastava *et al* (1976) show a minimum, whereas both the present work and the data of Rohr (1979) show a maximum. The absolute values of the present data are consistently lower than both previous measurements. For incident energies between 7.2 and 20 eV the agreement with Srivastava *et al* (1976) is excellent. At 7.2 eV, the agreement with the data of Rohr (1979) is also excellent but at 10 eV Rohr's data, as at 5 eV, is consistently higher at the smaller scattering angles. At 12 eV there is no other experimental work with which to compare.

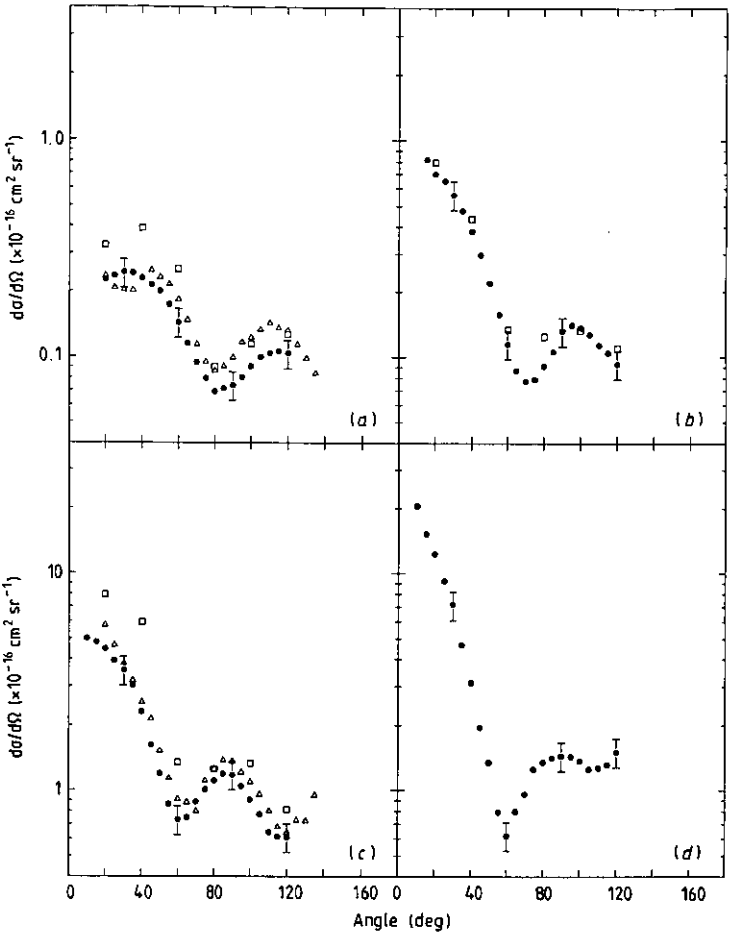

Figure 2. Differential cross section (10^{-16} cm^2 sr^{-1}) at (*a*) 5 eV, (*b*) 7.2 eV, (*c*) 10 eV, (*d*) 12 eV. ●, present work; △, Srivastava *et al* (1976); □, Rohr (1979).

At 30 eV the present data has the same general shape as that of Srivastava *et al* (1976), but as for 5 eV, the magnitude of the present cross section is consistently lower. At 40 and 50 eV there is reasonable agreement with Srivastava *et al* (1976) the major differences occurring for $\theta \geqslant 100°$ and in the region around $\theta = 40°$, where a minimum or inflection is observed in the present work before the cross section rises steeply as θ approaches 0°. The same feature has also been seen by Sakae *et al* (1989) at 75 eV (figure 4(*b*)), whose data concur with the present work. The most likely reason for the non-appearance of this feature in the data of Srivastava *et al* (1976) is the superior angular resolution of the apparatus used in the present work and that of Sakae *et al* (1989).

3.2. Integral and momentum transfer cross sections

Integral (σ_t) and momentum transfer (σ_m) cross sections have been derived from an extrapolation of the DCS to $\theta = 0°$ and 180° and the results are shown in table 2. Integral cross sections for electron impact on SF_6 have been reported by Srivastava *et al* (1976)

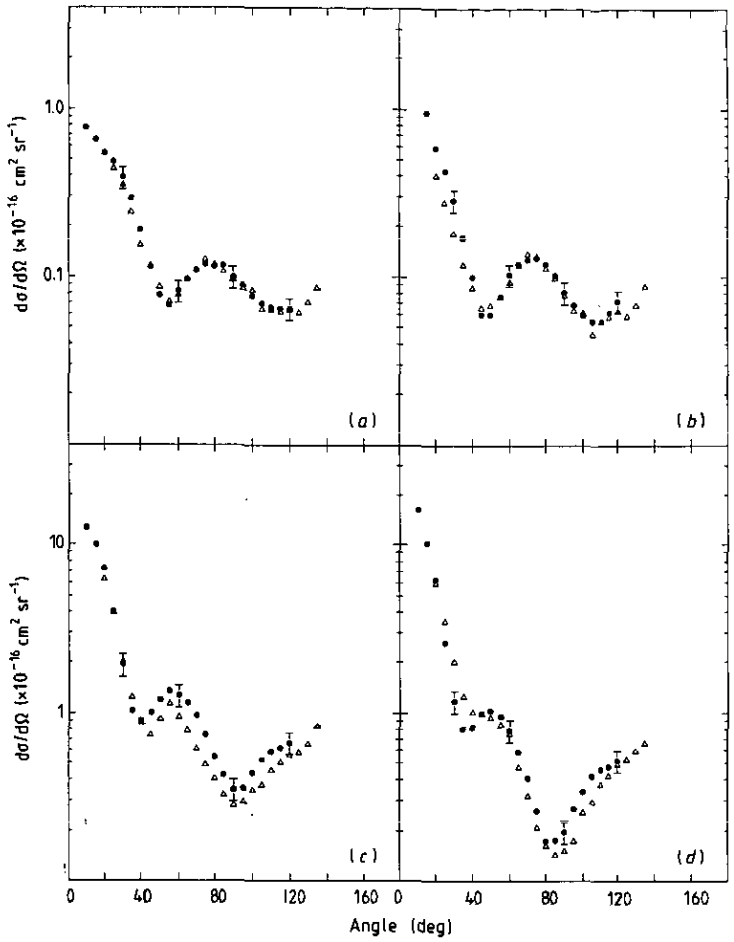

Figure 3. Differential cross section (10^{-16} cm^2 sr^{-1}) at (*a*) 15 eV, (*b*) 20 eV, (*c*) 30 eV, (*d*) 40 eV. ●, present work; △, Srivastava *et al* (1976).

and Sakae *et al* (1989) who also obtained values of σ_t from an extrapolation of their angular differential cross sections. The values of Srivastava *et al* (1976) have been recalculated using the renormalized differential cross sections (see section 3.1). Two theoretical calculations also exist, Dehmer *et al* (1978) and Gyemant *et al* (1980) and both are based on a multiple-scattering type calculation.

Two measurements have been made of the total cross section for electron impact on SF_6 by Kennerly *et al* (1979) and Dababneh *et al* (1988). It is possible to derive the total cross section from the integral cross section by addition of the total ionization and excitation cross sections. Figure 5 shows a plot of σ_t against incident electron energy. The ionization cross sections of Rapp and Englander-Golden (1965) have been added to the integral sections derived in the present work and to the results of Srivastava *et al* (1976), Sakae *et al* (1989), Dehmer *et al* (1978) and Gyemant *et al* (1980). No data is available with which to calculate the excitation integral cross section, but it is probable that its contribution is no larger than 5% of the total. The results of Kennerly *et al* (1979) are very similar to those of Dababneh *et al* (1988) and so have not been included for the sake of clarity. In figure 5, the agreement of the present work with

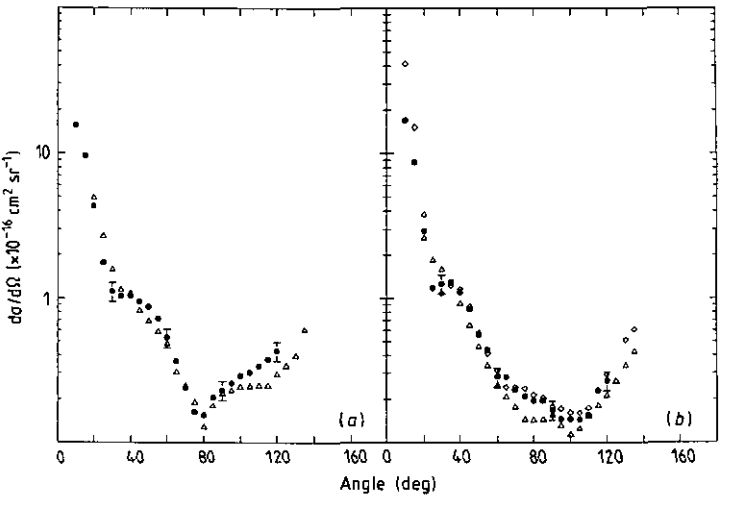

Figure 4. Differential cross section (10^{-16} cm^2 sr^{-1}) at (*a*) 50 eV, (*b*) 75 eV. ●, present work; △, Srivastava *et al* (1976); ◇, Sakae *et al* (1989).

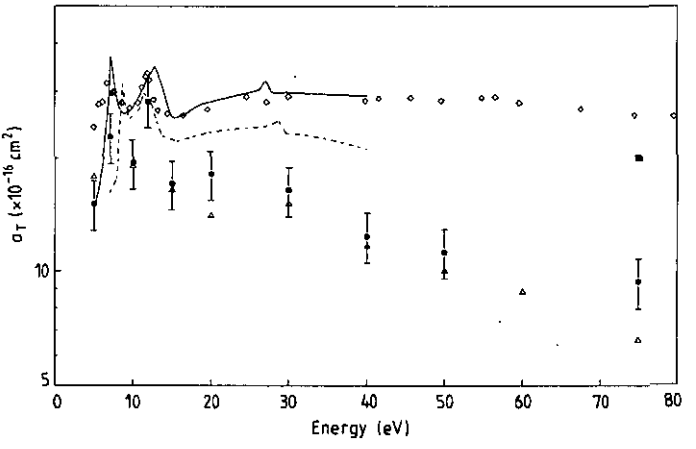

Figure 5. Total cross section (10^{-15} cm^2). Experiment: ●, present work; △, Srivastava *et al* (1976); ■, Sakae *et al* (1989); ▽, Dababneh *et al* (1988). Theory: ——, Dehmer *et al* (1978); - - - -, Gyemant *et al* (1980).

that of Srivastava *et al* (1976) is good and at 7.2 and 12 eV the present work shows a significant rise in the cross section. At 75 eV, the work of Sakae *et al* (1989) is notably higher than either the present work or that of Srivastava *et al* (1976) but is in good agreement with the direct σ_t measurements. The results of Kennerly *et al* (1979) and Dababneh *et al* (1988) and the calculations of Dehmer *et al* (1978) and Gyemant *et al* (1980) are also in reasonable agreement. Both calculations predict the presence of the two peaks near 7 and 12 eV, although at slightly different energies and intensities. In comparison with the values of σ_t determined from the present work and by Srivastava *et al* (1976), the measurements and calculation of Kennerly *et al* (1979), Dababneh *et al* (1988), Dehmer *et al* (1978) and Gyemant *et al* (1980) are consistently higher but are similar in shape.

The disagreement seen at the higher energies between the total cross section measurements and the theory with the values of σ_t derived from the present work and that of Srivastava *et al* (1976) can be explained by an examination of the differential cross section data, particularly at 75 eV. From figure 4(*b*), it can be seen that the data of Sakae *et al* (1989) is much higher at the smaller scattering angles than the present work or that of Srivastava *et al* (1976). There is a similar difference between the present work and that of Srivastava *et al* (1976) at 40 and 50 eV. Thus at the higher energies, the discrepancy in the values of σ_t appears to be due to a difficulty in accurately measuring the steeply rising differential cross section at the small scattering angles.

Apart from Srivastava *et al* (1976) and the single measurement of Sakae *et al* (1989), there have been no other reported measurements of the momentum transfer cross section in the energy range 5-75 eV. The momentum transfer data from these authors plus those calculated from the present work is shown in figure 6. As can be seen from table 2 a large proportion of the derived momentum transfer cross sections are calculated from the extrapolated values used to extend the differential cross section to 0° and 180°. Even so the agreement between the present data and that of Srivastava *et al* (1976) is good. The trend of σ_m is similar to that of σ_t. The cross section shows an increase at 7.2 and 12 eV and then falls away at 75 eV. As the calculation of σ_m is heavily weighted in favour of $\sigma(\theta) > 90°$, it is expected that the errors encountered in measuring $\sigma(\theta)$ for small scattering angles has a smaller effect on σ_m than σ_t.

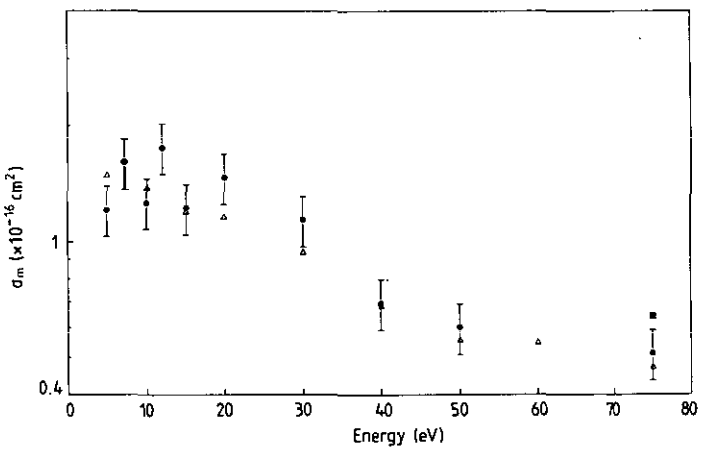

Figure 6. Momentum transfer cross section (10^{-15} cm^2). Experiment: ●, present work; △, Srivastava *et al* (1976); ■, Sakae *et al* (1989).

3.3. Resonance behaviour

Figures 5 and 6 show clear evidence of resonance enhancement of the cross section at 7 and 12 eV and figure 7 which shows the differential cross section at 20° as a function of energy also exhibits similar behaviour. The results of figure 7 are in good agreement with the work of Trajmar and Chutjian (1978), who measured the elastic differential cross section as a function of energy from 9 to 17 eV at scattering angles 20°, 60°, 90° and 135°. Rohr (1979) has made measurements of the elastic cross section in the 7 eV region but his results do not show the same increase at or around 7.2 eV.

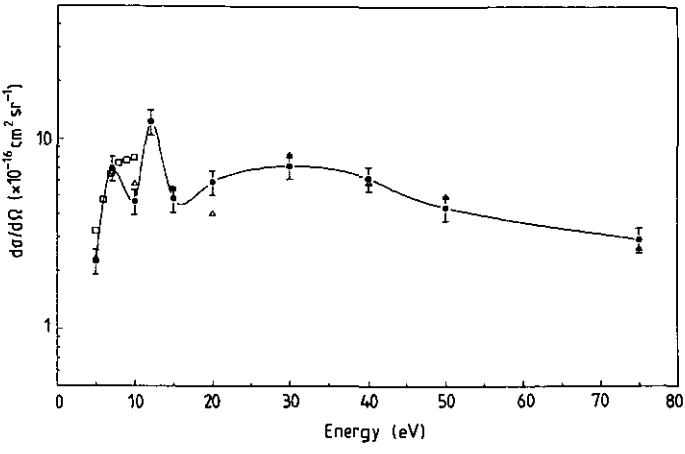

Figure 7. Differential cross section (10^{-16} cm^2 sr^{-1}) as a function of energy at 20°. —●—, present work; △, Srivastava *et al* (1976); □, Rohr (1979).

This may be due to a normalization error in the work of Rohr (1979) as at the lower scattering angles, where the largest enhancement is seen, the data are considerably higher than the present work and that of Srivastava *et al* (1976).

Dehmer *et al* (1978) and Gyemant *et al* (1980) have produced theoretical calculations for total electron scattering in which resonant behaviour has been observed. Both authors used a similar method based on a 'muffin tin' version of the multiple-scattering method, where the molecular field is partitioned into three regions. The major difference between the two calculations is in the construction of the potential seen by the scattered electron and number of partial waves used.

Dehmer *et al* (1978) have predicted the existence of four resonances and have given them the following orbital assignments; a_{1g} (2.1 eV not shown in figure 5), t_{1u} (7.2 eV), t_{2g} (12.7 eV) and e_g (27.0 eV) where (0, $\underline{4}$), (1, $\underline{3}$), (2, $\underline{4}$, 6) and (2, $\underline{4}$, $\underline{6}$) are the partial waves giving the biggest contribution to the cross section at the resonance energies. (The underlined l's denote the partial waves exhibiting the increase in phase at the resonance energies.) In addition, the calculations indicated that the two lowest-lying resonances, a_{1g} and t_{1u}, were molecular in origin, whereas the t_{2g} and e_g resonances were seen to stem from an 'atomic' d-type resonance associated with the sulphur atom. Gyemant *et al* (1980) also found evidence for the three highest resonances and their calculations also indicated that the t_{2g} and e_g resonances came from a d-resonance on the sulphur site. They further noted that the position and width of the resonances were highly dependent on the choice of potential.

Both theories show reasonable agreement with the works of Kennerly *et al* (1979) and Dababneh *et al* (1988). One major difference worth noting is the lack of evidence for the e_g resonance in the experimental data. From an analysis of the angular behaviour of the differential cross section data it is possible to judge which are the dominant partial waves at the resonance energies. For the first resonance a_{1g}, Dehmer *et al* (1978) have indicated that the dominant partial waves are $l = 0$ and 4. The differential cross section data of Rohr (1979) at 2.7 eV and the present data at 5 eV would seem to support this. It is surprising that the $l = 4$ partial wave should show a significant contribution at such a low energy and its presence may be due to exchange and polarization effects. At the second resonance t_{1u}, Dehmer *et al* (1978) suggest that the

dominant partial waves are $l = 1$ and 3 and the work of Gyemant *et al* (1980) shows substantial contributions from $l = 0$ and 1 partial waves. An inspection of the differential cross section at 7.2 eV (figure 2(*b*)) would appear to contradict this, as the behaviour indicates the presence of $l = 0$, 2 and 4. Finally the $l = 2$, 4 and 6 are calculated to be the principle partial waves for the t_{2g} resonance at 12 eV. The differential cross section shown in figure 2(*c*) does show a similar behaviour but the primary partial wave would appear to be $l = 2$. This is in agreement with Gyemant *et al* (1980) who show a rapidly rising contribution from the $l = 2$ partial wave at this energy.

4. Conclusion

Absolute elastic DCS measurements have been made for electron scattering from SF_6 and generally the agreement between the present data and previously published results is good. Integral and momentum transfer cross sections have been derived from the DCS measurements and have been compared with the data from previous experiments and theoretical calculations. Evidence is seen for resonance enhancement in the differential, integral and momentum transfer cross sections in line with previous measurements and theoretical calculations. Thus there now exists a validated set of experimental data for electron scattering from SF_6 which can be used for the normalization of inelastic data and as a guide to any further theoretical calculations.

Acknowledgments

The authors would like to thank Mr E J C Oldfield and Mr I Rangué for their invaluable technical assistance and the Physics Department for their support.

References

Andrick D and Bitsch A 1975 *J. Phys. B: At. Mol. Phys.* **8** 393
Brunt J N H, King G C and Read F H 1977 *J. Phys. B: At. Mol. Phys.* **10** 1289
Christophorou L G, James D R and Pai R Y 1982 *Applied Atomic Collision Physics* ed H S W Massey, E W McDaniel and B Bederson (New York: Academic) p 87
Chutjian A 1981 *Phys. Rev. Lett.* **46** 1511
Dababneh M S, Hseih Y F, Kauppila W E, Kwan C K, Smith S J, Stein T S and Uddin M N 1988 *Phys. Rev.* A **38** 1207
Dehmer J L, Siegel J and Dill D 1978 *J. Chem. Phys.* **69** 5205
Endo N and Kurogi Y 1980 *IEEE Trans. Electron Devices* **ED-27** 1346
Gyemant I, Varga Z S and Benedict M G 1980 *Int. J. Quantum Chem.* **17** 255
Johnstone W M and Newell W R 1989 *Proc. 16th Int. Conf. on the Physics of Electronic and Atomic Collisions (New York)* (Amsterdam: North-Holland) Abstracts p 280
Kanik I, McCollum D C and Nickel J C 1989 *J. Phys. B: At. Mol. Opt. Phys.* **22** 1225
Kennerly R E, Bonham R A and McMillan M 1979 *J. Chem. Phys.* **70** 2039
Khakoo M A and Trajmar S 1986 *Phys. Rev.* **34** 138
Newell W R, Brewer D F C and Smith A C H 1981 *J. Phys. B: At. Mol. Phys.* **14** 3209
Nesbet R K 1979 *Phys. Rev.* A **20** 58
Nickel J C, Zetner P W, Shen G and Trajmar S 1989 *J. Phys. E: Sci. Instrum.* **22** 730
Pitno R, Ramanthan K V and Babau R S 1987 *J. Electrochem. Soc.* **134** 165
Rapp D and Englander-Golder P 1965 *J. Chem. Phys.* **43** 1464
Register D F, Trajmar S and Srivastava S K 1980 *Phys. Rev.* A **21** 1134

Rohr K 1979 *J. Phys. B: At. Mol. Phys.* **12** L185
Sakae T, Sumiyoshi S, Murakami E, Matsumoto Y, Ishibashi K and Katase A 1989 *J. Phys. B: At. Mol. Opt. Phys.* **22** 1385
Srivastava S K, Chutjian A and Trajmar S 1975 *J. Chem. Phys.* **63** 2659
Srivastava S K, Tajmar S, Chutjian A and Williams W 1976 *J. Chem. Phys.* **64** 2767
Trajmar S and Chutjian A 1977 *J. Phys. B: At. Mol. Phys.* **10** 2943
Trajmar S and Register D F 1984 Experimental techniques for cross section measurements *Electron-Molecule Collisions* ed K Takayanagi and I Shimamura (New York: Plenum)
Trajmar S, Register D F and Chutjian A 1983 *Phys. Rep.* **97** 216